A Diverse Family of GPCRs Expressed in Specific Subsets of Nociceptive Sensory Neurons

Xinzhong Dong,[1] Sang-kyou Han,[2] Mark J. Zylka,[1] Melvin I. Simon,[2] and David J. Anderson[1,3,4]
[1] Division of Biology 216-76 and
[2] Division of Biology 147-75
[3] Howard Hughes Medical Institute
California Institute of Technology
Pasadena, California 91125

Summary

In vertebrates, peripheral chemosensory neurons express large families of G protein-coupled receptors (GPCRs), reflecting the diversity and specificity of stimuli they detect. However, somatosensory neurons, which respond to chemical, thermal, or mechanical stimuli, are more broadly tuned. Here we describe a family of approximately 50 GPCRs related to *Mas1*, called *mrgs*, a subset of which is expressed in specific subpopulations of sensory neurons that detect painful stimuli. The expression patterns of *mrgs* thus reveal an unexpected degree of molecular diversity among nociceptive neurons. Some of these receptors can be specifically activated in heterologous cells by RFamide neuropeptides such as NPFF and NPAF, which are analgesic in vivo. Thus, *mrgs* may regulate nociceptor function and/or development, including the sensation or modulation of pain.

Introduction

Dorsal root (spinal) ganglia contain diverse subpopulations of primary sensory neurons (Scott, 1992). These include muscle afferent sensory neurons that project to motoneurons in the ventral spinal cord and cutaneous afferent sensory neurons that project to the dorsal spinal cord. Within the subclass of cutaneous afferent sensory neurons, there is further diversification into low-threshold mechanoceptors and high-threshold nociceptors. This latter category includes neurons that respond to a variety of noxious thermal, mechanical, or chemical stimuli that cause acute pain (Willis and Coggeshall, 1991). In addition, such nociceptive neurons mediate chronic pain associated with inflammatory responses or nerve injury (so-called "neuropathic" pain).

Nociceptive sensory neurons exhibit further diversification (reviewed in Caterina and Julius, 1999; Hunt and Mantyh, 2001). For example, these neurons can be subdivided into so-called Aδ and C-fibers based on their spike-firing thresholds and the presence or absence of myelination, respectively. C-fibers, in turn, can be subclassified into those that express proinflammatory neuropeptides, such as Substance P, and a "nonpeptidergic" subclass that does not (Molliver et al., 1997; Bennett et al., 1998; Stucky and Lewin, 1999); these subclasses project to distinct laminae in the dorsal spinal

cord (reviewed in Snider and McMahon, 1998). In addition, C-fibers innervate a variety of peripheral targets including the skin, gut, vasculature, and muscle. Within these targets, such small-diameter sensory fibers show several categories of morphologically distinct nerve endings (Fundin et al., 1997; Rice et al., 1997). The molecular bases of these various aspects of phenotypic diversity among somatosensory neurons are largely unknown.

In recent years, our understanding of nociception and its modulation has been advanced by the identification and functional analysis of signaling molecules expressed in nociceptive sensory neurons (Akopian et al., 1996a). These molecules include the vanilloid receptor VR1, purinergic receptors such as P2X3, and the TTX-insensitive sodium channel (reviewed in Caterina and Julius, 1999). Another family of signaling molecules, which play a prominent role in various sensory systems, are G protein-coupled receptors (GPCRs). Several GPCRs are expressed in nociceptive sensory neurons. These include the NPY receptors, the Protease-Activated receptors (PARs), the bradykinin receptor (reviewed in Hunt and Mantyh, 2001), opiate receptors (Dado et al., 1993), and prostaglandin receptors (Donaldson et al., 2001). More recently, a GPCR expressed in nociceptors, termed R35, has been identified, although its function is unknown (Friedel et al., 2001).

Here we report the identification of a large GPCR subfamily comprising almost 50 members that are related to MAS1 (Young et al., 1986), called *Mas-related genes* (*mrgs*). A subset of these genes, including *mrgAs* and *mrgD*, is specifically expressed in *Griffonia simplicifolia* lectin IB4^{+} sensory neurons, a subpopulation that includes cutaneous nociceptors and which has been implicated in "neuropathic" (nerve injury-induced) pain (Malmberg et al., 1997). The expression of *mrgAs* and *mrgD* thus reveals an unexpected degree of molecular diversity among nociceptive sensory neurons. Their expression in these neurons further suggests that they could be involved in pain sensation or its modulation. In heterologous cells, mrgA1 and A4 can be activated by the RFamide neuropeptides NPFF and NPAF, respectively, which produce long-lasting analgesic effects when injected intraspinally (reviewed in Panula et al., 1999). These data, and the specificity of expression of *mrgAs* and *mrgD*, suggest that ligands for these receptors may include neuropeptides that modulate pain sensitivity.

Results

Identification of *mrgA*, *mrgB*, and *mrgC* Subfamilies
Previous studies have shown that in mouse embryos lacking the bHLH transcription factor *Neurogenin1* (*Ngn1*) (Ma et al., 1996), most trkA^{+} neurons, which include the nociceptive subclass, fail to be generated (Ma et al., 1999). We exploited this mutant phenotype to isolate genes specifically expressed in such neurons by subtracting cDNAs from neonatal wild-type and *Ngn1^{−/−}*

[4] Correspondence: wuwei@caltech.edu

DRG (see Experimental Procedures). Genes expressed in the former but not the latter cDNA population should be specific to trkA$^+$ neurons. Consistent with this idea, the screen yielded several signaling molecules known to be involved in nociceptor functions, including the capsaicin receptor VR1 (Caterina et al., 1997), CGRP, and SNS, the sensory neuron-specific, tetrodotoxin-insensitive sodium channel α subunit (Akopian et al., 1996b).

The screen also identified at least five previously unknown genes. Among these, one encoded a receptor protein with seven transmembrane segments, a characteristic of GPCRs. This GPCR shows highest homology (35% identity) to MAS1 (Young et al., 1986). It also shares significant homology (30%–35% identity) with two other mammalian GPCRs, called Mas-related gene 1 (*mrg1*) (Monnot et al., 1991) and rat thoracic aorta (RTA) (Ross et al., 1990). Based on its homology with the *Mas* gene family, we named this receptor *mrgA1* (*Mas-related gene A1*). Further screening of murine DRG cDNA and BAC libraries led to the identification of seven additional closely related (70%–80% identity) full-length genes (*mrgsA2–8*) (Figure 1A). Since *mrgA* genes are highly homologous to each other (see Supplementary Table S1A, Supplemental Data, below) and have certain characteristic conserved residues, they define a subfamily of the MAS family of GPCRs.

Computer searches (see Experimental Procedures) using mrgA1 as the query sequence revealed 14 additional members of the murine *mrgA* subfamily (Figure 1B). In addition to this subfamily, two closely related *mrg* subfamilies, called *mrgB* and *mrgC*, were also discovered by such database searches (Figure 1B). The *mrgB* subfamily contains 13 genes, whereas *mrgC* has 14 members. The percent sequence identity within each of these subfamilies is >50% (see Table S1A, Supplemental Data, below). Strikingly, all 14 *mrgC* members appear to be pseudogenes (Figure 1B, "Ψ"), as they contain multiple premature stop codons, frameshift mutations, or both. Thus, the *mrgA*, *mrgB*, and *mrgC* subfamilies comprise almost 50 sequences, of which 27 encode intact ORFs.

Searches of the Celera (Venter et al., 2001) and public (I.H.G.S., 2001) genomic sequence databases, using both BLAST (Altschul et al., 1990) and Hidden Markov Models (HMMs; Eddy, 1998), revealed four closely related (~50% identity) full-length human genes and at least nine human pseudogenes (Figure 1B, *Hs.mrgX1*, etc.). Although the human genes appear to be more similar to the murine *mrgA* subfamily than the *mrgB* subfamily in the phylogenetic tree (Figure 1B, *hmrgX1-4*), in the absence of clear orthologous pairs we currently refer to them as *Hs.mrgX* genes. In addition to the *mrgA*, *B*, and *C* subfamilies, a number of additional *Mas1*-related orphan GPCRs were identified by this search, including those we refer to as *mrgs D–G* (Figure 1B). Most of these sequences have clear human orthologs (Figure 1B and Table S1B, Supplemental Data, below). Altogether, we identified almost 31 murine and 8 human intact coding sequences belonging to this family of GPCRs.

Mrg receptors have short (3–21 amino acid) N termini, with no apparent signal peptide, which are predicted to be located extracellularly. The transmembrane domains and intracellular domains are highly conserved, sug-

gesting that the receptors have a shared function. The most divergent regions of mrgA-family receptors appear localized to the extracellular loops (Figures 1A, E1, E2, etc.), suggesting that these receptors recognize different ligands, or the same ligand but with different affinities. Interestingly, we identified 12 single nucleotide polymorphisms in the *mrgA1* coding sequence between murine strains C57BL/6J and 129/SvJ. These 12 changes resulted in six amino acid substitutions, all of which were either conservative, or which substituted residues expressed at the same position by other family members.

A large mouse genomic contig was built by analyzing overlapping BAC clones containing mrgA sequences (Figure 1C). There are seven *mrgA* genes, including three pseudogenes, residing in this contig. Such clustering is a common feature of GPCR-encoding gene families (Xie et al., 2000). Strikingly, all of the human *mrg* genes (with the exception of *Mas1* and *mrg1*) are located on chromosome 11, which also contains nearly 50% of all human olfactory receptors genes (Glusman et al., 2001). All of the *mrgA* genes in the murine BAC contig (Figure 1C) encode intact ORFs with N-terminal methionines, like many other GPCR-encoding genes. Using the Celera mouse genome database, sequences flanking each *mrgA* coding region were obtained and analyzed. This analysis revealed that at least nine *mrgA* genes have L1 retrotransposon sequences located ~650 bp downstream of their coding sequences (Figure 1B, L1).

mrgAs and *mrgD* Are Expressed in Subsets of Primary Sensory Neurons

To determine whether *mrgAs* are expressed in DRG neurons, in situ hybridization using dioxygenin-labeled riboprobes was performed for the eight *mrgA* cDNA clones initially isolated from the DRG cDNA and BAC libraries. This analysis revealed that all eight *mrgAs* (*mrgA1–8*) are expressed in subsets of sensory neurons, in wild-type neonatal DRG (Figures 2B–2I). Importantly, the expression of all eight *mrgAs* was virtually absent in DRGs of *Ngn1*$^{-/-}$ animals (Figure 2J and data not shown), consistent with the design of the subtractive hybridization screen. Among the eight *mrgA* clones examined, *mrgA1* has the widest expression within sensory neurons in neonatal DRGs (13.5%). Other *mrgAs* are only expressed in several cells per DRG section (ranging from 0.2%–1.5% of DRG neurons). This differential abundance may explain why only *mrgA1* was isolated in the original screen. No obvious differences in the expression patterns of *mrgA1–8* were noticed in DRGs from different axial levels.

The expression of *mrgAs* in sensory neurons appears highly specific, in that in situ hybridization signals have not been detected in any other tissue of the body except trigeminal ganglia (Figure 2K, arrowhead, and data not shown). Like the *mrgA* genes, *mrgD* was also specifically expressed in a subset of DRG sensory neurons, and was not detectable in any other tissue except trigeminal ganglia in neonatal animals (Figure 2L, arrowhead; see below). In contrast, expression of other *mrgs*, including *mrgB1-5*, *Mas1*, *mrgE*, *mrgF/RTA*, *mrgG*, and *GPR90*, was not detectable in DRGs (data not shown). Preliminary Northern blot analysis using *Hs.mrgX1* and *X2* as
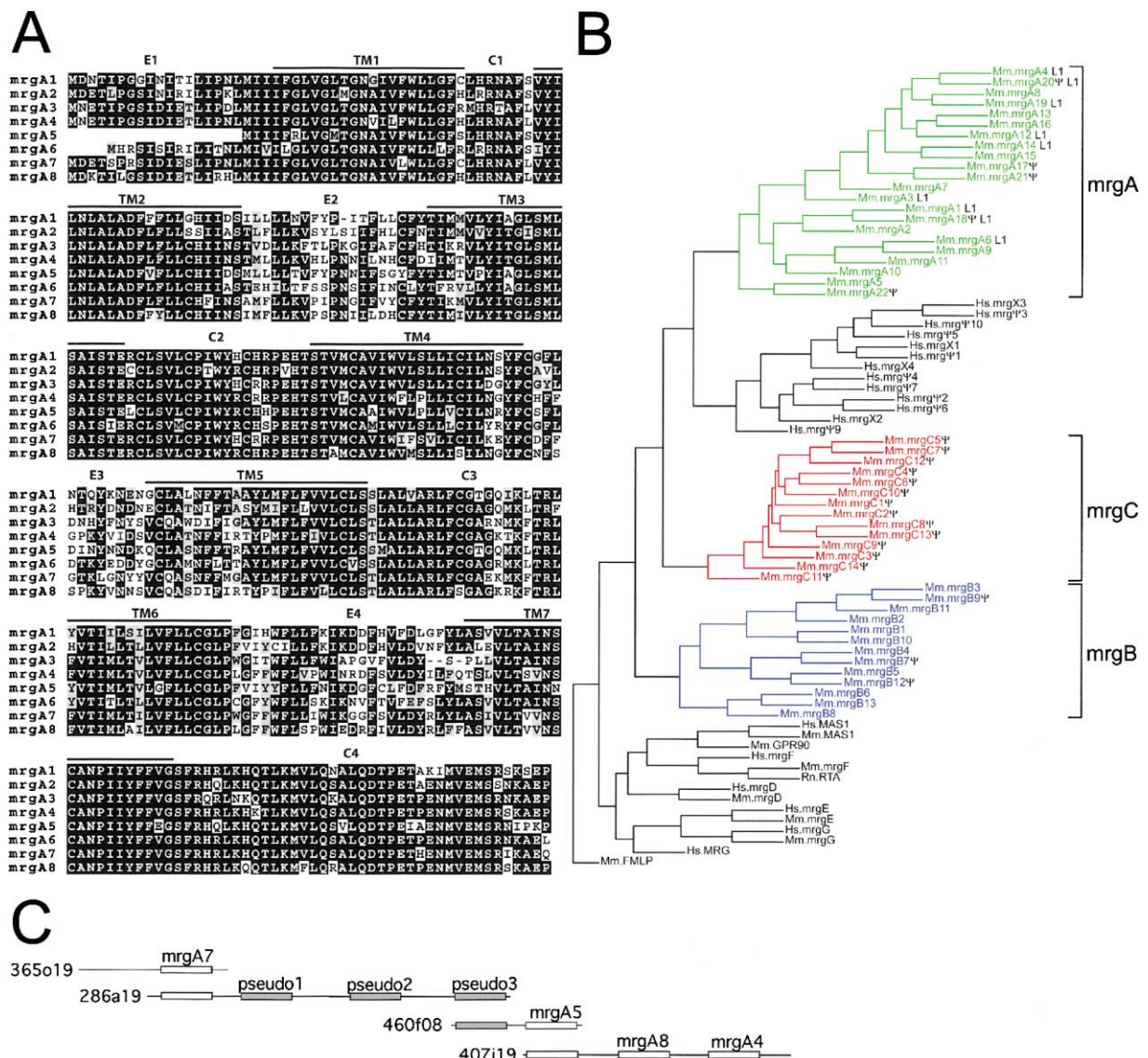
Figure 1. *mrgA* Genes Are Members of a Large Family of G Protein-Coupled Receptors

(A) Alignment of amino acid sequences of mrgA1-A8. Residues shaded in black are identical in >50% of the predicted proteins; similar residues are highlighted in gray. The predicted transmembrane (TM1-TM7), extracellular (E1-E4), and cytoplasmic (C1-C4) domains are indicated.

(B) Phylogenetic analysis of murine (Mm) and human (Hs) mrg family members. The protein sequences were aligned using CLUSTALW (Thompson et al., 1994). Mouse formyl peptide receptor 1 (Mm.FMLP) was used as the outgroup. The dendrogram was generated with the PHYLUP software package using the Neighbor-Joining method and 1,000 bootstrap trials. The horizontal length of the branches is proportional to the number of amino acid changes. Vertical distances are arbitrary. Murine *mrg* genes with retrotransposon sequences ~650 nt 3′ of their stop codon are highlighted (L1). Ψ, predicted pseudogenes.

(C) Chromosomal organization of one mouse *mrg* gene cluster deduced from analysis of overlapping BAC clones. The cluster contains four intact ORFs and three pseudogenes.

probes failed to reveal detectable expression in a panel of 12 different human tissues; however these did not include DRG (not shown).

Different *mrgAs* Are Expressed in Largely Nonoverlapping Subsets of Sensory Neurons
The in situ hybridization data obtained using individual *mrgA* probes raised the question of whether these receptors are expressed by distinct or overlapping subsets of sensory neurons. Double-label in situ hybridiza-

tion studies using probes labeled with digoxigenin and fluorescein indicated that in neonates, many neurons expressing *mrgA3* or *mrgA4* coexpress *mrgA1* (Figures 3A–3F, arrowheads). In addition to strongly labeled *mrgA4*^{+} cells (Figure 3E, arrowhead), the fluorescent in situ hybridization signals for *mrgA4* using tyramide amplification included dots within nuclei that were circumscribed by the cytoplasmic expression of *mrgA1* mRNA, as detected by fast red (Figure 3F, arrow). Such dots of *mrgA4* expression were not observed using the
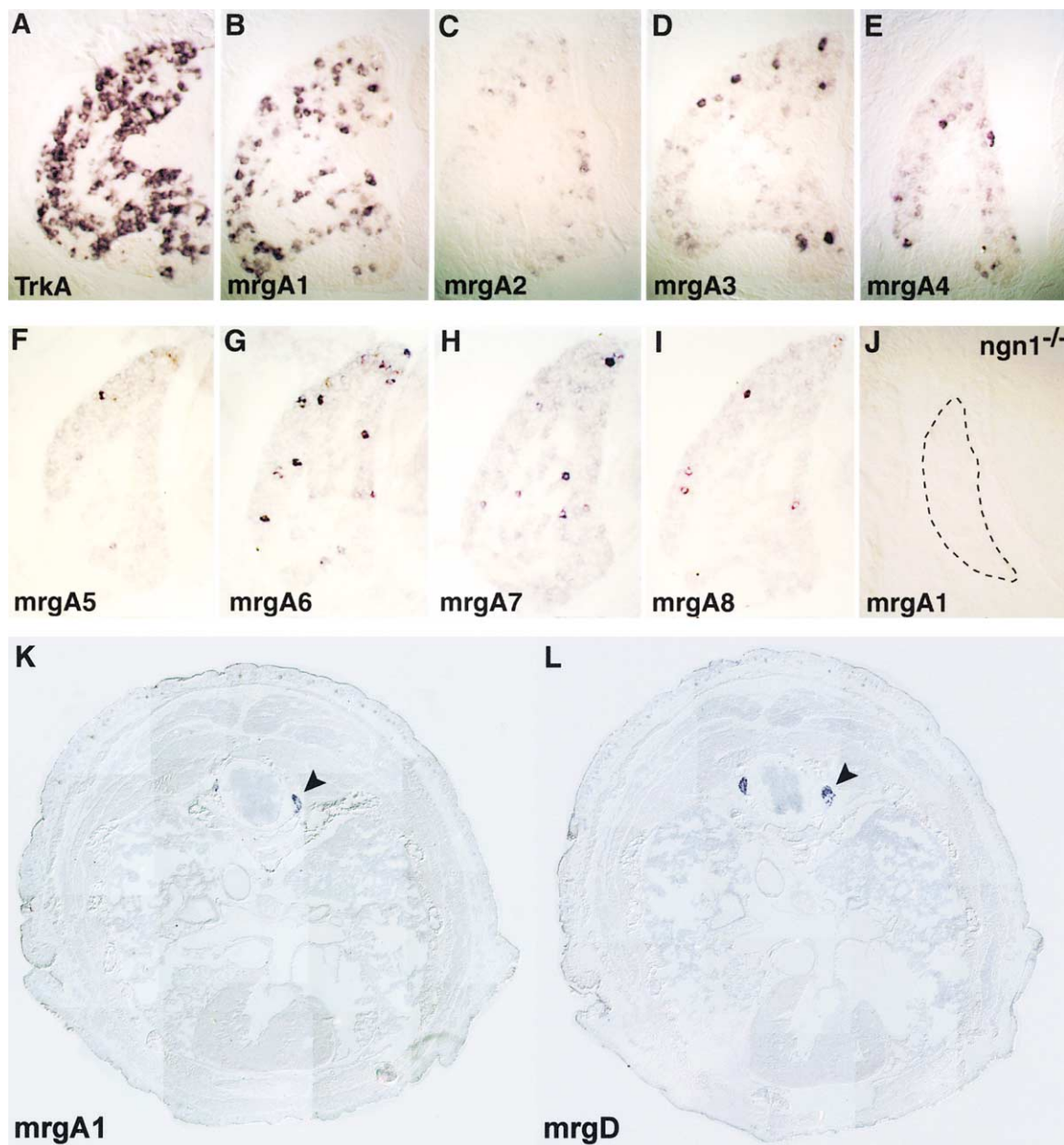
Figure 2. *mrgAs* Are Expressed in Subsets of Nociceptive Sensory Neurons

(A–I) In situ hybridization with cRNA probes detecting *trkA* (A) and *mrgA1-A8* (B–I).

(J) *mrgA1* Expression is eliminated in *Ngn1⁻/⁻* mice, as is expression of other *mrgA* genes (not shown). Remaining DRG neurons are present in the area delimited by the dotted line (not shown; see Ma et al., 1999).

(K and L) Cross-sections through the trunk region of neonatal mice hybridized with probes for *mrgA1* (K) and *mrgD* (L). Arrowheads indicate specific expression in the DRG. Expression was not detected in any other tissue, at this or at other axial levels (data not shown).

less sensitive fast red detection method, and were only observed in the nuclei of *mrgA1⁺* cells. Similar intra-nuclear dots have previously been observed in studies of pheromone receptor gene expression, and have been suggested to represent sites of transcription (Pantages and Dulac, 2000). Other *mrgA* probes gave insufficiently strong signals to be used in such double-labeling experiments. Nevertheless, the results for *mrgA1*, *3*, and *4* suggested that those neurons that express the rarer *mrgA* genes (*mrgA2-8*) are a subset of those that ex-

press *mrgA1* in newborn animals. In adults, however, *mrgA1* is expressed by a smaller subset of sensory neurons and only partially overlaps the expression of other *mrgAs* (see below).

To address the question of whether *mrgsA2-A8* are expressed in the same or in different neurons, we compared the number of neurons labeled by single probes to that labeled by a mixture of all seven probes (Buck and Axel, 1991). Approximately 3-fold more neurons (4.5% versus 1%) were labeled by the mixed *mrgsA2-A8* probe
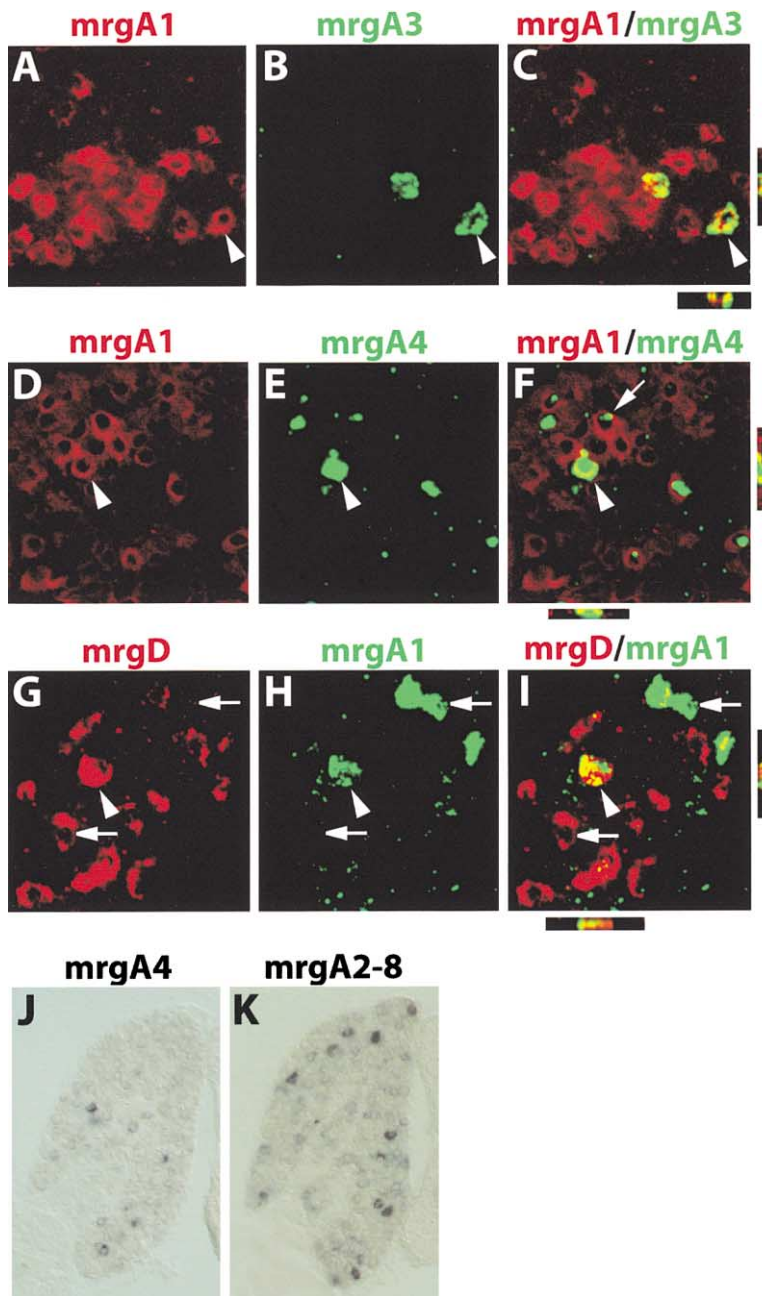
Figure 3. Partially Overlapping Expression of Different *mrgAs* in Neonatal Sensory Neurons

(A–C) Double label in situ hybridization with *mrgA1* (A, red) and *A3* (B, green).

(D–F) Double labeling with *mrgA1* (D) and *mrgA4* (E). In neonates, cells expressing *mrgA3* or *A4* are a subset of those expressing *mrgA1* (C and F, arrowheads). However, in adults, *mrgA1* is mostly nonoverlapping with other *mrgAs*.

(G–I) Double label in situ with *mrgA1* and *mrgD*. Expression is mostly nonoverlapping (I, arrows), although some double-positives are seen (I, arrowhead). Vertical bars (C, F, and I) represent a z-series viewed along the *y* axis, horizontal bars a z-series viewed along the *x* axis, confirming double-labeling of the same cells.

(J and K) Comparison of in situ experiments using a single *mrgA4* probe (J) versus a mixture of seven *mrgA* probes (K).

than by an individual probe (*mrgA4*; Figures 3J and 3K), indicating that these genes are not all coexpressed in the same population of neurons. However, the percentage of neurons labeled by the mixed probe (4.5%) was less than the sum of the percentage of neurons labeled by each of the seven individual probes (6.6%). This observation, and the fact that a higher signal intensity was observed in individual neurons using the mixed probe than using a single probe, suggests that there is some overlap in the expression of *mrgA2-A8*, at least at birth.

We next examined the relationship between neurons expressing *mrgA1* and *mrgD*. In neonatal DRG, there was a partial overlap between *mrgA1*+ and *mrgD*+ cells (Figures 3G–3I, arrowheads). Approximately 15% (118/786) of neurons expressing either *mrgA1* or *mrgD* coex-

pressed both genes. 34% (118/344) of *mrgA1*+ cells coexpressed *mrgD*, while 26.7% (118/442) of *mrgD*+ cells coexpressed *mrgA1*. This partial overlap at birth, however, is transient, and the expression of *mrgAs* and *mrgD* becomes segregated in adulthood (see below). A similar pattern of transient coexpression followed by segregation has been observed for other receptors expressed in subsets of DRG sensory neurons, such as trkA and c-ret (Molliver et al., 1997).

Mrgs Are Expressed in a Subset of trkA+ Neurons at Birth

The lack of expression of *mrgAs* in DRGs from *Ngn1*−/− mice is consistent with the idea that they are expressed in trkA+ sensory neurons, which include nociceptors
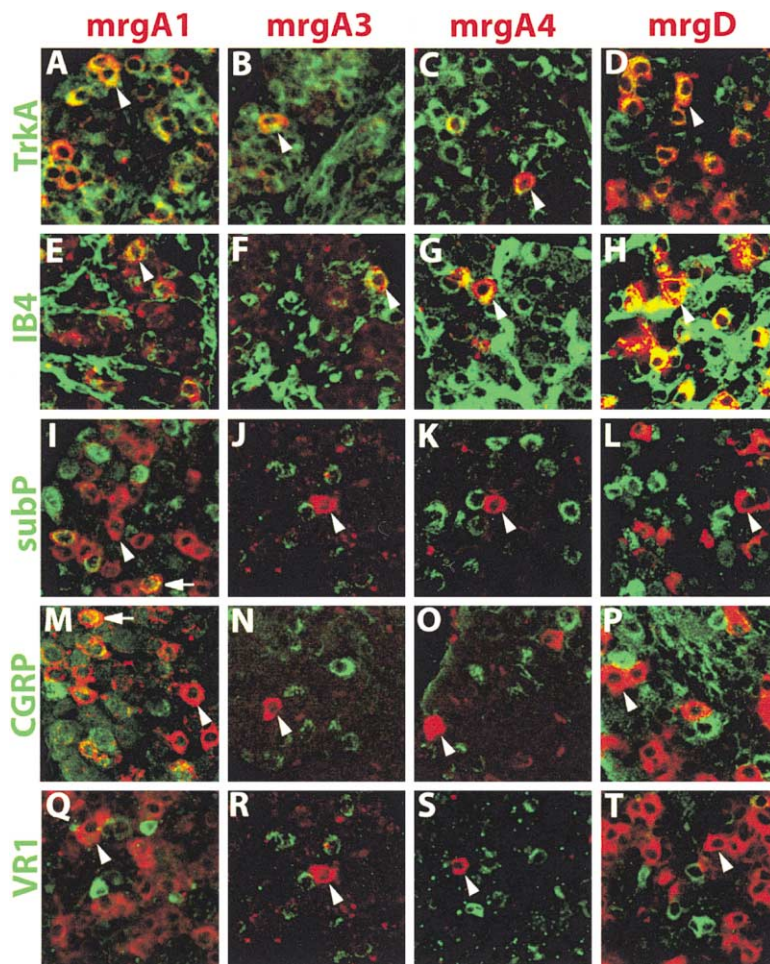
Figure 4. Expression of *mrgs* in Neonatal DRG

1 μm confocal microscope optical sections of P0 DRG hybridized in situ with the indicated *mrg* probes (red), combined with fluorescent antibody detection of trkA (A–D), substance P (SubP, I–L), CGRP (M–P), VR1 (Q–T), or staining with fluorescent lectin IB4 (IB4; E–H) (green). IB4 labels blood vessels in addition to neurons in DRG. Arrows in (I) and (M) indicate a minor subset of *mrgA1*^{+} neurons that coexpresses Substance P and CGRP.

(McMahon et al., 1994; Snider and Silos-Santiago, 1996). Furthermore, the distribution of *mrgA1*^{+} cells was similar to that of *trkA*^{+} cells on adjacent sections (Figures 2A and 2B). To directly determine whether *mrgA* genes are expressed in trkA^{+} cells, in situ hybridization was performed on neonatal DRG for *mrgA1*, *A3*, and *A4* in conjunction with immunolabeling using anti-trkA antibodies. These experiments confirmed that *mrgAs* are indeed coexpressed in trkA^{+} neurons (Figures 4A–4C, arrowheads) at birth. Similar results were obtained for *mrgD* (Figure 4D, arrowhead). These data suggest that *mrgAs* and *mrgD* are specifically expressed in a population of sensory neurons that contains nociceptive as well as other neuronal subtypes.

To determine whether *mrgs* are expressed in more restricted subsets of such neurons, additional double-labeling experiments were carried out. Combined fluorescent labeling for isolectin B4 (IB4) together with in situ hybridization with *mrgA1*, *A3*, *A4*, and *mrgD* probes suggested that these receptors are expressed by IB4^{+} neurons (Figures 4E–4H, arrowheads), an assignment confirmed by analysis of adult DRG (see below). This result implies that *mrgs* are expressed by nonpeptidergic nociceptive neurons that project to lamina IIi (Snider and McMahon, 1998). Consistent with this assignment, the majority (90%) of *mrgA1*[+], and all *mrgA3*[+], *mrgA4*[+], and *mrgD*^{+} cells, lack substance P expression (Figures

4I–4L, arrowheads). Similarly, all *mrgD*^{+} cells, and many *mrgA*^{+} cells, do not express CGRP (Figures 4M–4P, arrowheads), another neuropeptide expressed by C-fiber nociceptors.

Recent studies have provided evidence for the existence of two neurochemically and functionally distinct subpopulations of IB4^{+} nociceptors: those that express the vanilloid receptor VR1 (Caterina et al., 1997), and those that do not (Michael and Priestley, 1999; Stucky and Lewin, 1999). Strikingly, in situ hybridization with *mrgA* or *D* probes combined with anti-VR1 antibody immunostaining indicated that the *mrgA1*, *A3*, *A4*, and *D*-expressing cell populations were mutually exclusive with VR1^{+} cells (Figures 4Q–4T, arrowheads). In summary, these expression data suggest that *mrgA* and *D* genes are expressed in the subclass of nonpeptidergic sensory neurons that are IB4^{+} and VR1^{−} (Figure 5CC).

Expression of *mrgAs* and *mrgD* in Adult DRG Identifies At Least Two Distinct Subsets of IB4^{+}, VR1^{−} Sensory Neurons

The finding that *mrgAs* and *mrgD* are expressed in trkA[+], IB4^{+} sensory neurons at birth is consistent with the fact that the latter two markers are coexpressed by nonpeptidergic sensory neurons in neonates (Molliver et al., 1997). During the second postnatal week, however, the IB4^{+} neurons downregulate expression of trkA,
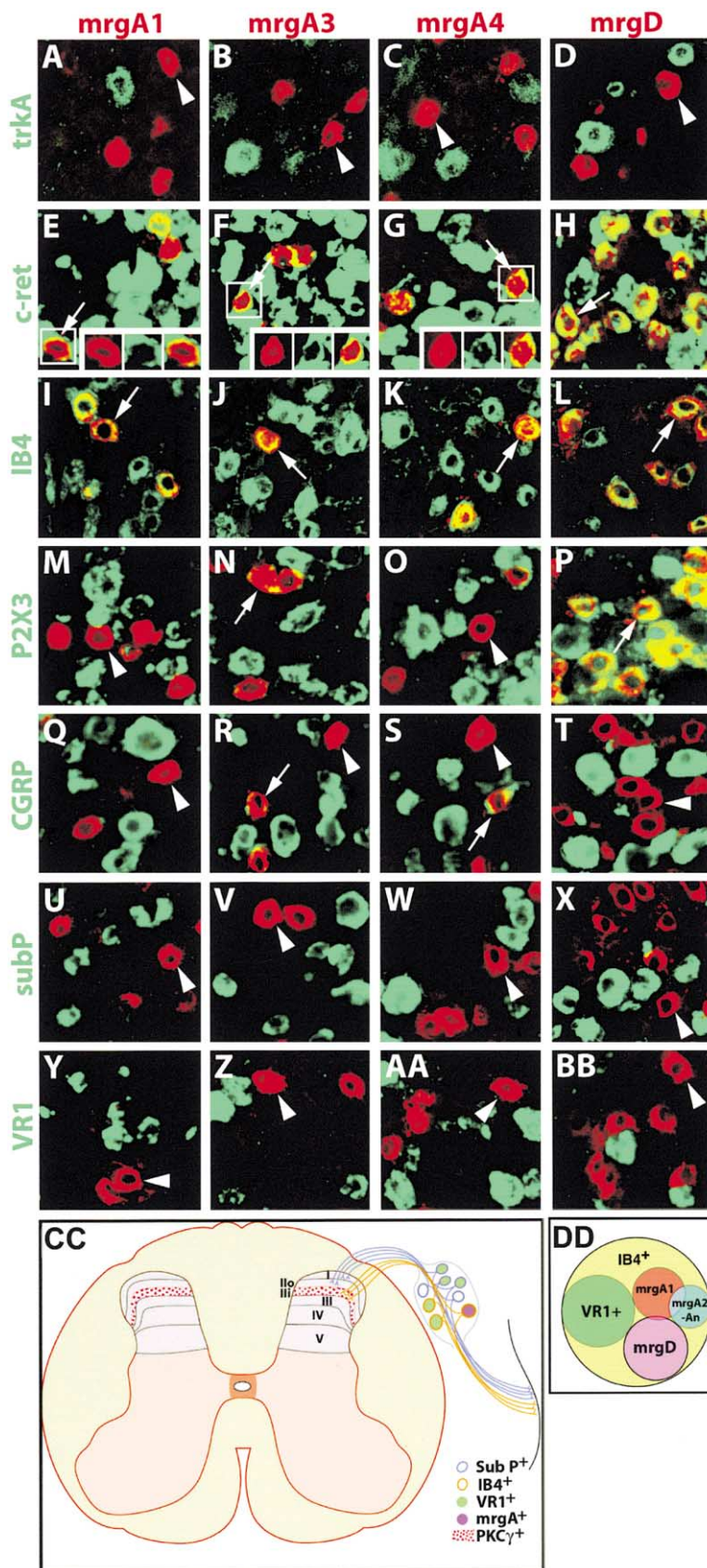
Figure 5. Expression of *mrgs* in adult DRG

Shown are 1 μm confocal microscope optical sections of adult DRG processed for double-label in situ hybridization with the indicated markers. In all panels, *mrgs* are in red, the countermarkers in green. All countermarkers are cRNA in situ hybridization probes except fluorescent IB4 lectin and anti-trkA antibody. Arrowheads indicate single-positive cells, arrows double-positive cells. Expression of *mrgAs* is restricted to neurons that express lower levels of *c-ret* mRNA than do *mrgD*-expressing neurons (E–G, arrows). Insets show the boxed cells at higher magnification with the red and green channels separated. (CC) Schematic illustrating restriction of *mrgA* (and *mrgD*) expression to nonpeptidergic, IB4+, *VR1*- sensory neurons (orange with purple fill) that project to lamina IIi, marked by expression of PKCγ (magenta stippling). (DD) Venn diagram illustrating the different subsets of IB4+, VR1- DRG neurons defined by expression of *mrgAs* and *mrgD*. The drawing is a conservative estimate of the number of subsets; their sizes are not proportional. For simplicity, all *mrgAs* except *A1* are condensed into a single group, although there is likely relatively little overlap between these *mrgAs* (see Figures 3J and 3K).

and become dependent on the neurotrophic factor GDNF, whose receptor, c-ret, they continue to express (Molliver et al., 1997). To determine whether expression of *mrgs* is maintained in the trkA$^+$ subpopulation, or rather the c-ret$^+$/IB4$^+$ population, we performed a series of double-labeling experiments on DRG from adult (4 week postnatal) mice.

Expression of both *mrgAs* and *mrgD* was maintained in IB4$^+$ neurons in adulthood (Figures 5I–5L arrows). All *mrgD$^+$* neurons coexpressed IB4, as did the majority (~90%) of *mrgA$^+$* cells. As expected from these data, the *mrgs* no longer colocalized with trkA in adult DRGs (Figures 5A–5D, arrowheads). Consistent with their expression in IB4$^+$ cells, 100% of *mrgD$^+$* cells strongly coexpressed *c-ret* (Figure 5H, arrow). Similarly, the majority (~93%) of *mrgA$^+$* cells were *c-ret$^+$* (Figures 5E–5G, arrows). However, the level of *c-ret* expression was consistently lower in the *mrgA$^+$* cells than in the *mrgD$^+$* cells, and was often restricted to the perimeter of the cell body (Figures 5E–5G, insets; cf. Figure 5H, arrow). These data suggested that *mrgAs* and *mrgD* might be expressed by distinct subsets of IB4$^+$ neurons, which differ quantitatively in their level of *c-ret* expression. Double-labeling experiments with *mrgA* versus *mrgD* probes in adult DRGs confirmed that these receptors are expressed in nonoverlapping populations of neurons (not shown). *MrgD$^+$* neurons coexpressed the purinergic receptor *P2X3* (Chen and McConnell, 1995) (Figure 5P, arrow), consistent with the fact that this receptor is known to be mostly restricted to the IB4$^+$ population (Bradbury et al., 1998). In contrast, most *mrgA$^+$* cells did not coexpress *P2X3* (Figures 5M–5O, arrowheads).

As was the case in neonates, *mrgA$^+$* and *mrgD$^+$* cells did not coexpress the neuropeptide *Substance P* (Figures 5U–5X), and *mrgD$^+$* cells were also negative for *CGRP* (Figure 5T, arrowhead). In contrast, approximately 50% of *mrgA$^+$* cells were *CGRP$^+$* (Figures 5R and 5S, arrows), consistent with the fact that a subset of IB4$^+$ cells are known to express this neuropeptide (Bradbury et al., 1998). The vanilloid receptor *VR1* continued to be excluded from both the *mrgA$^+$* and *mrgD$^+$* subpopulations (Figures 5Y–5BB), as was the case at birth. These data confirm that expression of *mrgs* is restricted in adults to a subset of IB4$^+$ sensory neurons that are *VR1$^-$*, as suggested by the data from neonatal animals (Figure 5CC). Moreover, our data reveal two distinct subsets of neurons within the IB4$^+$, *VR1$^-$* population: *mrgA$^+$* neurons are *c-ret^{low}* and mostly *P2X3$^-$*, while *mrgD$^+$* cells are *c-ret^{high}* and *P2X3$^+$* (Figure 5DD). Furthermore, while in neonates there is overlap between *mrgA1* and other *mrgAs*, in adults the *mrgAs* are largely nonoverlapping (not shown). Therefore, the *mrgA$^+$* subset is likely further subdivided into different subpopulations expressing different *mrgsAs* (Figure 5DD).

The expression of *mrgAs* and *mrgD* in IB4$^+$ cells suggests that these receptors are present in a population of sensory neurons that terminate in lamina IIi ((Bennett et al., 1998); Figure 5CC), which includes nociceptors (Molliver et al., 1997). Another classical criterion for sensory neuron subtype is cell body diameter: nociceptive sensory neurons typically have the smallest cell somata of all neurons in the DRG (Scott, 1992). Although an accurate measurement of absolute cell somata diameters for *mrg$^+$* neurons is precluded by the tissue distor-

tion that accompanies in situ hybridization, we performed pairwise comparisons of the average diameter of *mrgA1$^+$*, *A3$^+$*, *A4$^+$*, and *mrgD$^+$* neurons with that of *VR1$^+$* neurons (whose cell diameters are characteristic of nociceptors (Tominaga et al., 1998)), on the same double-labeled sections (Figures 5Y–5BB). This analysis indicated that the average diameter of *mrgA1$^+$* (19.7 ± 2.94 μm), *mrgA3$^+$* (20.7 ± 1.7 μm), *mrgA4$^+$* (19.9 ± 2.47 μm), or *mrgD$^+$* (21.9 ± 1.98 μm) cells is slightly but significantly less than that of *VR1$^+$* neurons (24.3 ± 4.94 μm; p<.0064 or less for all pairwise comparisons between *mrg$^+$* and *VR1$^+$* neurons). These data indicate that *mrg$^+$* cells fall within the size range characteristic of small-diameter nociceptive sensory neurons.

mrgA1 and A4 Can Function as Receptors for Neuropeptides

The structure of the proteins encoded by *mrg* genes suggests that they function as receptors. As a first step toward testing this hypothesis, we sought to determine whether these GPCRs could be activated by any known ligands. To this end, we cloned selected *mrgA* genes, including *mrgA1* and *mrgA4*, into a eukaryotic expression vector and transfected them into human embryonic kidney (HEK) 293 cells. By fusing GFP to the C termini of the *mrgA* coding sequences, we were able to visualize the intracellular distribution of the receptors and confirm their membrane integration in the transfected cells (see Supplemental Figure S1D, Supplemental Data, below). To increase the sensitivity of the assay, in some experiments the mrgA-GFP fusion proteins were expressed in HEK 293 cells modified to express Gα$_{15}$, which couples GPCRs to a signal transduction pathway leading to the release of intracellular free Ca^{2+} (Offermanns and Simon, 1995). This calcium release can be monitored ratiometrically using Fura-2 as a fluorescent indicator dye (Tsien et al., 1985) (see Figures S1A–C, Supplemental Data). This heterologous expression system has been previously used to identify ligands for taste receptors (Chandrashekar et al., 2000).

Because mrgAs exhibit the highest sequence similarity to peptide hormone receptors, we screened approximately 45 candidate peptides for their ability to activate mrgA1 using this intracellular Ca^{2+}-release assay. At a concentration of 1 μM, numerous neuropeptides produced some level of activation of *mrgA1*-expressing cells (Figure 6A). These included ACTH, CGRP-I and -II, NPY, and somatostatin (SST). Nevertheless, many other peptide hormones did not activate mrgA1, including angiotensins I–III and neurokinins A and B, α-MSH, and γ$_2$-MSH (Figure 6A and data not shown). *mrgA1*-expressing cells were only very weakly activated by ecosanoid ligands such as prostaglandin-E1 and arachidonic acid (data not shown). Nontransfected HEK-Gα$_{15}$ cells were strongly activated by PACAP, VIP, and ATP, and weakly activated by secretin, endothelin, and helodermin. No responses to bradykinin were detected in HEK-Gα$_{15}$ cells, although the parental HEK 293 cells showed responses to this peptide as previously reported (Anderson et al., 1995).

The most efficient responses in *mrgA1*-expressing HEK cells were elicited by RFamide peptides, including FLRF and the molluscan cardioactive neuropeptide

FMRFamide (Price and Greenberg, 1977) (Phe-Met-Arg-Phe-amide) (Figures 6A and S1C, Supplemental Data). We therefore tested two mammalian RFamide peptides, NPAF and NPFF, which are cleaved from a common propeptide precursor (Vilim et al., 1999). The response of *mrgA1*-expressing cells to NPFF at 1 μM was similar to that seen with FMRFamide, while that to NPAF was significantly lower (Figure 6A). mrgA1 was also weakly activated by two other RFamide ligands, γ_1-MSH and schistoFLRF (data not shown).

In order to examine further the specificity of activation of mrgA1 and A4, we retested the top candidate ligands emerging from the initial screen on these same receptors expressed in HEK 293 cells lacking $G\alpha_{15}$. MrgA1 and A4 expressed in this system retained responses to RFamide peptides at a concentration of 1 μM (Figures 6B and 6C). This suggests that mrgAs may act in HEK 293 cells via G_q or $G_{i/o}$. The response of *mrgA1*-expressing HEK 293 cells to NPFF was lower than that to FLRF (Figure 6B), and there was no response to NPAF. Conversely, *mrgA4*-expressing cells responded to NPAF, but not to NPFF or FLRF (Figure 6C). In both cases, the response to NPY seen in $G\alpha_{15}$-expressing cells (Figure 6A) was lost completely, while those to CGRP-II and ACTH were considerably diminished.

In order to determine the lowest concentrations of RFamide ligands capable of activating mrgA1 and A4, we performed dose reponse experiments in HEK-$G\alpha_{15}$ cells, which afforded greater sensitivity (Figures 6D and 6E). These experiments indicated that mrgA1 could be activated by FLRF at nanomolar concentrations (Figure 6D, squares; EC$_{50}$ $\sim$20 nM), and by NPFF at about an order of magnitude higher concentration (Figure 6D, circles; EC$_{50}$ $\sim$200 nM), whereas NPAF was much less effective. In contrast, mrgA4 was well activated by NPAF (Figure 6E, triangles; EC$_{50}$ $\sim$60 nM), and much more weakly activated by FLRF and NPFF. Neither receptor was activated well by RFRP-1, -2, or -3, a series of RFamide ligands produced by a different precursor (Hinuma et al., 2000). These data therefore confirmed that mrgA1 and mrgA4 display different selectivities toward different RFamide ligands in this system. By contrast, these receptors responded similarly to ACTH (EC$_{50}$ $\sim$60 and $\sim$200 nM for mrgA1 and A4, respectively; data not shown).

Finally, given the sequence similarity between mrgA receptors and MAS1, we tested the responsiveness of cells expressing exogenous *Mas1* to NPFF, NPAF, and FLRF. MAS1 showed a profile distinct from both mrgA1 and mrgA4 (Figure 6F): like mrgA1, it was activated by NPFF at a similar concentration of the peptide (EC$_{50}$ $\sim$400 nM), but unlike mrgA1, it was poorly activated by FLRF. In contrast to mrgA4, MAS1 did not respond well to NPAF. We did not detect responses in *MAS1*-expressing cells exposed to Angiotensins I and II, ligands which have been previously reported to activate this receptor (Jackson et al., 1988). Nor did MAS1 respond to ACTH. Thus, *MAS1*, *mrgA1*, and *mrgA4* expressed in this heterologous system are all activated by RFamide family ligands, but with differing ligand sensitivities and selectivities (Table 1). Importantly, nontransfected HEK-$G\alpha_{15}$ cells were not activated by any of these RF-amide ligands (Figures 6D–6F, open symbols).

MrgAs Exhibit Characteristic Activation and Desensitization Kinetics to Neuropeptide Ligands

To further characterize the response of mrgA receptors to their preferred neuropeptide ligands, we examined their activation and desensitization kinetics. Addition of 1 μM FLRF and NPAF to *mrgA1*- and *mrgA4*-transfected HEK-$G\alpha$15 cells, respectively, elicited a rapid rise in [Ca^{2+}]$_i$, with peak responses achieved within 10–20 s following agonist stimulation (Figures 6G and 6H). The responses were sustained for $>$500 s, after which they slowly returned to baseline (not shown). To determine whether the activation kinetics or ligand selectivity were affected by the GFP fusion at the C terminus of the receptors, the experiments were repeated using V5 epitope-tagged or untagged forms of mrgA1 and A4 in both HEK-$G\alpha_{15}$ and parental HEK 293 cells. No differences in relative selectivity or activation kinetics were found in response to FLRF, NPFF, NPAF, and ACTH in these experiments (not shown).

Finally, to determine whether mrgAs undergo desensitization in response to their preferred ligands, HEK 293 cells expressing untagged forms of *mrgA1* or *mrgA4* were challenged with multiple pulses of 1 μM FLRF or NPAF, respectively. The successive application of these ligands in both cases led to progressively reduced peak responses, indicative of densensitization (Figures 6I and 6J; see insets) (Kobilka, 1992). Following each successive ligand application and washout, responses returned to baseline in $\sim$200 s, slightly faster than observed with HEK-$G\alpha_{15}$ cells (see above). Recovery from desensitization was observed after ligand washout and incubation for 15–20 min (Figures 6I and 6J; break in abscissa). Continuous exposure to the ligands for $>$20 s resulted in adaptation, seen as a fast increase in [Ca^{2+}]$_i$ followed by a slower deactivation (not shown). Similar results were obtained using GFP- or V5-epitope-tagged forms of the receptors (not shown). Taken together, these data indicate that mrgA1 and A4 exhibit activation and desensitization kinetics in response to their preferred neuropeptide ligands, a characteristic feature of GPCRs (Kobilka, 1992).

Discussion

Vertebrate peripheral chemosensory neurons express large families of GPCRs (Buck and Axel, 1991; Dulac and Axel, 1995; Troemel et al., 1995; Matsunami and Buck, 1997; Adler et al., 2000; Matsunami et al., 2000), reflecting the diversity of ligands that these sensory systems have evolved to detect. In contrast, primary somatosensory neurons are thought not to specifically discriminate amongst different chemical ligands, but rather respond to polymodal stimuli (thermal, chemical, mechanical) by virtue of broadly tuned receptors such as VR1 (Tominaga et al., 1998). Here we describe a gene family consisting of close to 50 MAS1-related GPCRs, the expression of which reveals an unanticipated degree of molecular diversity among DRG sensory neurons. The specific expression of *mrgAs* and *mrgD* in a subset of IB4$^+$ sensory neurons further suggests that these receptors may be involved in the sensation or modulation of pain, and could therefore provide targets for antinociceptive drugs.
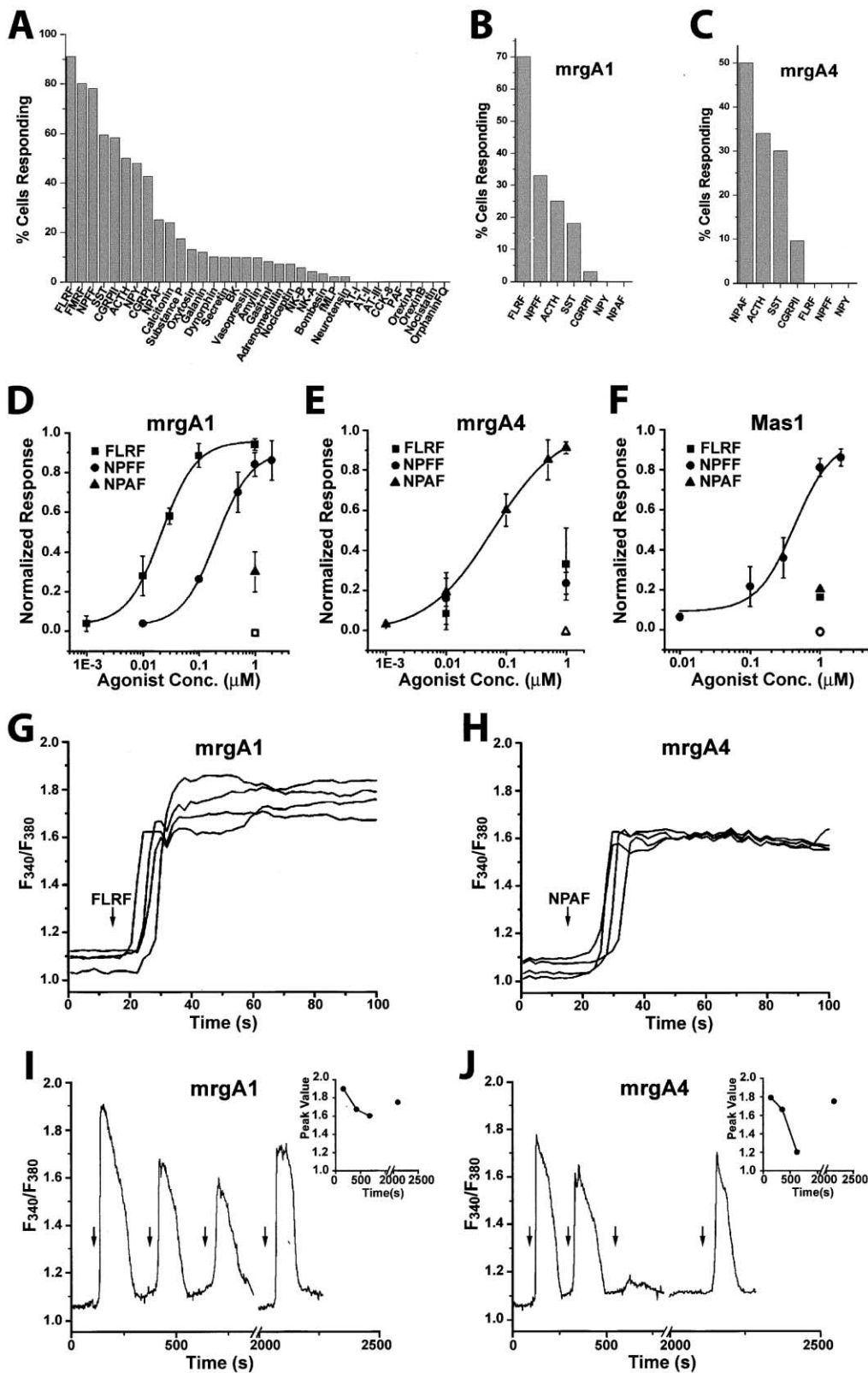
Figure 6. Activation of mrgA Receptors Expressed in Heterologous Cells by Neuropeptide Ligands

(A) HEK-Gα_{15} cells (Offermanns and Simon, 1995) expressing mrgA1 were tested with the indicated ligands at a concentration of 1 μM. The data indicate the mean percentages of GFP-positive (i.e., transfected) cells showing calcium responses. None of the agonists indicated showed any responses through endogenous receptors in untransfected cells.

Table 1. Selectivity of Activation of Mas-Related GPCRs by RFamide Ligands in HEK-Gα_{15} Cells

Receptor	Ligand		
	FLRF	NPFF	NPAF
mrgA1	+++	++	+/−
mrgA4	+/−	+/−	+++
MAS1	+/−	++	+/−

Relative efficacy of activation of the indicated receptors by the indicated ligands is shown. For quantification, see Figure 6. "+++" indicates 10 nM < EC$_{50}$ < 100 nM; "++" indicates 100 nM < EC$_{50}$ < 500 nM; "+/−" indicates weak response seen at 1 μM. For details see Figure 6.

Structure and Evolution of the *mrg* Family

The murine *mrg* family of GPCRs contains three major subfamilies (*mrgA*, *B*, and *C*), each consisting of >10 highly duplicated genes. In contrast, we were able to identify only four intact human *mrgX* sequences. The remaining nine human *mrg* sequences appear to be pseudogenes. Why do mice have more *mrg* genes than do humans? In the case of odorant receptors, the high percentage of pseudogenes in humans (~70%; Mombaerts, 1999) may reflect the decreased reliance of *H. sapiens* on olfaction in relation to other sensory modalities, such as vision. In the case of the *mrgs*, it may reflect differences in nociception and/or mechanoception between mice and humans, perhaps related to the presence or absence of fur and whiskers. However, the presence of L1 retrotransposon elements near several *mrg* genes raises the possibility that their expansion may have been driven by L1-mediated transduction (Brosius, 1999; Goodier et al., 2000). If so, then the apparently higher level of ongoing retrotransposon activity in mice compared to humans (I.H.G.S., 2001) could also account for the greater size of the murine *mrg* gene family. However, the observation that strain-specific polymorphisms in these genes (C57BL/6J versus 129/SvJ) are either silent, or result in conservative amino acid substitutions, argues against the idea that the diversity of *mrg* genes in mice has no functional relevance and simply reflects expansion of "selfish DNA."

mrgAs and *D* Are Expressed in a Specific Subset of Sensory Neurons that Includes Nociceptors

Some clues to the function of mrgs may be provided by the specific subpopulation of neurons in which they are expressed. *MrgA1-8* and *D* are all expressed by IB4$^+$, c-ret$^+$ sensory neurons (Molliver et al., 1997; Bennett et al., 1998). These neurons primarily send their central projections to lamina IIi (Snider and McMahon, 1998), which has been implicated in neuropathic pain (Malmberg et al., 1997). These data suggest that *mrgAs* and *mrgD* are likely expressed in nociceptive sensory neurons. In support of this assignment, nociceptors tend to be the smallest-diameter neurons in the DRG (Scott, 1992), and the average cell body diameters of *mrgA*$^+$ and *mrgD*$^+$ cells are similar to, or smaller than, that of VR1$^+$ neurons, which are known nociceptors (Tominaga et al., 1998; Caterina et al., 2000). However, *mrgA*$^+$ and/or *mrgD*$^+$ neurons may also include low threshold cutaneous mechano- or thermoreceptors. These functions are not mutually exclusive: *mrg*$^+$ sensory neurons may be polymodal.

Strikingly, both *mrgAs* and *mrgD* are expressed by VR1$^-$ neurons within the IB4$^+$ population. VR1 is activated by both noxious thermal and chemical stimuli (Tominaga et al., 1998), but in vivo is dispensable for the detection of noxious mechanical stimuli (Caterina et al., 2000). While VR1$^+$ neurons may detect such mechanical stimuli via other receptors, it is also possible that *mrgA*$^+$ and/or *mrgD*$^+$ neurons detect stimuli of different modalities than are detected by VR1$^+$ neurons, including noxious mechanical stimuli. Genetic ablation or silencing of *mrgA*- and *mrgD*-expressing neurons may permit their assignment to specific sensory modalities, irrespective of the function of mrgs themselves.

Expression of *mrgs* Defines a Distinct Axis of Diversity among IB4$^+$ Sensory Neurons

The expression of *mrgAs* and *D* reveals an unanticipated degree of diversity among IB4+, VR1$^-$ sensory neurons (Figure 5DD). It is currently not clear what aspect of cellular or functional diversity this molecular heterogeneity underlies. The *mrgD*$^+$ subpopulation coexpresses *P2X3*, while *mrgA*$^+$ neurons mostly do not. *MrgD*$^+$ and *mrgA*$^+$ neurons may therefore have different physiological properties. The IB4$^+$ population is known to contain both unmyelinated (C-fibers) and small, thinly myelinated (Aδ) neurons (Jackman and Fitzgerald, 2000), but the relationship of these physiological properties to *mrg* expression remains to be determined.

Even further heterogeneity among IB4$^+$, VR1$^-$ neurons is implied by the potential expression of up to 17 different *mrgA* genes. Interestingly, the peripheral nerve endings of IB4$^+$ fibers in skin and whisker pads exhibit significant anatomical diversity, including so-called penicillate endings, bush endings, cluster endings, and free nerve endings (Fundin et al., 1997; Rice et al., 1997).

(B and C) Ligand selectivity of mrgA1 (B) and mrgA4 (C) expressed in HEK cells lacking Gα_{15}. The cells were exposed to ligands at a concentration of 1 μM as in (A).

(D–F) Dose-response curves for mrgA1 (D), mrgA4 (E), and MAS1 (F) expressed in HEK-Gα_{15} cells to selected RFamide neuropeptides. Each data point represents the mean ± SEM of at least three independent determinations; at least 20 GFP$^+$ cells were analyzed for each determination. Responses at each ligand concentration were normalized to the maximal response subsequently elicited by a 5 μM concentration of the optimal ligand (FLRF, NPAF, and NPFF in D, E, and F, respectively). Open symbols indicate lack of a response in nontransfected HEK-Gα_{15} cells to the peptides identified by the corresponding closed symbols.

(G–J) Activation and desensitization kinetics of mrgA1 and mrgA4 in response to their preferred neuropeptide ligands. (G and H) Single cell [Ca^{2+}]$_i$ transients recorded in response to application of 1 μM of the indicated ligands (arrows). Line traces are derived from several representative individual HEK-Gα_{15} cells expressing GFP-tagged forms of the indicated receptors. Similar results were obtained with untagged forms of these receptors (not shown). (I and J) Densensitization kinetics of untagged mrgA1 and mrgA4 in HEK 293 cells. Insets show the decline in peak responses following repeated application of ligands (arrows). Responses returned to normal within 15–20 min (break in abscissa).

The structure of such endings also varies according to the peripheral target, such as dermal layer, type of hair follicle, blood vessels, etc. There are currently no molecular correlates of such diversity. The ability to mark *mrg*-expressing neurons with genetically encoded axonal tracers (Mombaerts et al., 1996) should afford a means of relating their expression to such anatomical, as well as physiological, axes of sensory neuron diversity, and may provide further clues to the function of these receptors.

mrgAs Encode Probable Neuropeptide Receptors

The structure of mrgAs suggests that they function as receptors. Although a similar conclusion has been drawn for other orphan GPCRs expressed in peripheral sensory neurons (Buck and Axel, 1991; Dulac and Axel, 1995; Matsunami and Buck, 1997; Adler et al., 2000; Matsunami et al., 2000), it has with a few exceptions (Zhao et al., 1998; Chandrashekar et al., 2000) been difficult to demonstrate this directly. Here we have shown that mrgA1 and A4 can act as neuropeptide receptors when expressed in heterologous cells. Although we do not claim to have identified the authentic ligand(s) for these receptors, the nature of the molecules that activate them may provide some clues as to their selectivity. Specifically, mrgA1 and A4 were optimally activated by RFamide neuropeptides, such as FMRFamide, FLRFamide, NPFF, and NPAF. In contrast, mrgA1 was not activated by formyl-Met-Leu-Phe, which lacks an amidated C-terminal phenylalanine. These data suggest that mrgA1 and A4 may be receptors for RFamide-family neuropeptides, if not for NPFF and NPAF themselves. However, the fact that ACTH activated mrgA1 and A4 with equal efficacy as NPFF and NPAF, respectively, raises the possibility that the authentic ligands for these receptors are peptides unrelated to RFamides.

Binding sites for NPAF/NPFF analogs have been detected on primary sensory neuron fibers in the dorsal horn of the spinal cord (Gouarderes et al., 1996; Gouarderes et al., 2000). Furthermore, injection of NPFF analogs into the spinal cord produces long-lasting analgesia in several chronic pain models (reviewed in Panula et al., 1999). These data are consistent with the idea that MrgA1 and A4 could serve as receptors for these RFamide neuropeptides, and may modulate nociception, in vivo. However, two other human candidate GPCRs for NPAF and NPFF unrelated to mrgAs have been identified, called hNPFF1 and hNPFF2 (Bonini et al., 2000; Elshourbagy et al., 2000; Hinuma et al., 2000). Rat NPFF2 is activated by NPAF and NPFF in HEK-G$_{\alpha15}$ cells more strongly than are mrgA1 and A4, and unlike the latter receptors is not activated by ACTH (our unpublished data). RT-PCR experiments indicate that rNPFF2 is expressed in DRG (Bonini et al., 2000), and we have confirmed this in neonatal mouse DRG by in situ hybridization (M.J.Z., unpublished data). Whether the same neurons coexpress *rNPFF2* and *MrgAs* is not yet clear. Thus, while some primary sensory neurons clearly express receptors for NPFF/NPAF (Rebeyrolles et al., 1996; Askwith et al., 2000), the gene(s) encoding these receptors in vivo remain to be defined.

The Significance of *mrg* Sequence Diversity

The finding that mrgA1 and A4 can serve as receptors for neuropeptides begs the question of the reason for the diversity of the *mrg* gene family. One possibility is that this diversity reflects different affinities for unknown mammalian neuropeptides. Thus far, only four RFamide pre-propeptide precursors—those encoding NPFF/NPAF (Perry et al., 1997; Vilim et al., 1999), Prolactin-Releasing Peptide (PrRP) (Hinuma et al., 1998), RFRP (Hinuma et al., 2000), and KiSS (Ohtaki et al., 2001)—have been described in mammals. By contrast, the *C. elegans* genome contains over 20 genes encoding more than 50 different RFamide neuropeptides (Nelson et al., 1998; Li et al., 1999). Perhaps there are many more such neuropeptides to be discovered in mammals.

An alternative is that the diversity of mrg receptors might reflect different affinities for a single, or small number of, ligands, rather than different specificities that discriminate amongst a larger number. For example, neurons expressing different mrgs might respond to a common modulator(s) of peripheral nociceptor sensitivity, but with different affinities. Such a mechanism could, for example, allow graded regulation of a population of functionally equivalent neurons. It is even conceivable that mrgs function as axon guidance molecules, as has been demonstrated for odorant receptors in olfactory sensory neurons (Wang et al., 1998). In that system, the diversity of odorant receptors is thought to reflect a graded series of affinities for guidance molecules expressed on target cells (Wang et al., 1998). These possibilities are not mutually exclusive; if the olfactory GPCRs can play a dual role as receptors for small molecule ligands and as determinants of axon targeting, it could be true for other diverse families of GPCRs expressed in peripheral sensory neurons as well. Clearly, the identification of the mrg family raises far more questions than it answers. It should, however, open new avenues for the exploration of nociceptor development and function.

Experimental Procedures

Molecular Cloning of *mrgA* Family

PCR-amplified cDNAs from wild-type and Ngn1$^{-/-}$ DRG were used as tester and driver, respectively, in the PCR-Select subtractive hybridization protocol (Clontech). Details of the procedure are available (see Supplemental Data). Additional members of the mouse *mrg* family and human *mrgs* were identified bioinformatically using TBLASTN and the Celera mouse and human (Venter et al., 2001) sequence databases. 26 ORFs identified in this manner were verified by high-fidelity PCR amplification of mouse genomic DNA or human BAC clones and sequencing. These verified sequences have been deposited in GenBank (see Accession Numbers, below). Additional unverified sequences were used in the construction of the phylogenetic tree (Figure 1B) and are available (see Supplemental Data).

In Situ Hybridization and Immunohistochemistry

Nonisotopic in situ hybridization on frozen sections was performed as previously described using cRNA probes (Ma et al., 1996; Perez et al., 1999). Eight *mrgAs*, five *mrgBs*, and *mrgD* were used as probes. At least ten DRGs were analyzed to count the number of neurons positive for each probe. Details of double-labeling procedures are available (see Supplemental Data).

Calcium Imaging

HEK 293 cells were obtained from the ATCC. The HEK-G$_{\alpha15}$ cell line stably expressing G$_{\alpha15}$ was provided by Aurora Biosciences Corporation. Details of growth and transfection procedures are

available (see Supplemental Data). Calcium imaging using Fura-2 AM (Molecular Probes) was carried out using a continuous perfusion apparatus essentially as described in Tsien et al. (1985) and Chandrashekar et al. (2000). Details are available (see Supplemental Data).

Supplemental Data

Additional data are available on the *Cell* website (http://www.cell.com/cgi/content/full/106/5/619/DC1).

References

Adler, E., Hoon, M.A., Mueller, K.L., Chandrashekar, J., Ryba, N.J., and Zuker, C.S. (2000). A novel family of mammalian taste receptors. Cell *100*, 693–702.

Akopian, A.N., Abson, N.C., and Wood, J.N. (1996a). Molecular genetic approaches to nociceptor development and function. Trends Neurosci. *19*, 240–246.

Akopian, A.N., Sivilotti, L., and Wood, J.N. (1996b). A tetrodotoxin-resistant voltage-gated sodium-channel expressed by sensory neurons. Nature *379*, 257–262.

Altschul, S.F., Gish, W., Miller, W., Myers, E.W., and Lipman, D.J. (1990). Basic local alignment search tool. J. Mol. Biol. *215*, 403–410.

Anderson, L., Alexander, C.L., Faccenda, E., and Eidne, K.A. (1995). Rapid desensitization of the thyrotropin-releasing hormone receptor expressed in single human embryonal kidney 293 cells. Biochem. J. *311*, 385–392.

Askwith, C.C., Cheng, C., Ikuma, M., Benson, C., Price, M.P., and Welsh, M.J. (2000). Neuropeptide FF and FMRFamide potentiate acid-evoked currents from sensory neurons and proton-gated DEG/ENaC channels. Neuron *26*, 133–141.

Bennett, D.L., Michael, G.J., Ramachandran, N., Munson, J.B., Averill, S., Yan, Q., McMahon, S.B., and Priestley, J.V. (1998). A distinct subgroup of small DRG cells express GDNF receptor components and GDNF is protective for these neurons after nerve injury. J. Neurosci. *18*, 3059–3072.

Bonini, J.A., Jones, K.A., Adham, N., Forray, C., Artymyshyn, R., Durkin, M.M., Smith, K.E., Tamm, J.A., Boteju, L.W., Lakhlani, P.P. (2000). Identification and characterization of two G protein-coupled receptors for neuropeptide FF. J. Biol. Chem. *275*, 39324–39331.

Bradbury, E.J., Burnstock, G., and McMahon, S.B. (1998). The Expression of P2X3 Purinoreceptors in Sensory Neurons: Effects of Axotomy and Glial-Derived Neurotrophic Factor. Mol. Cell. Neurosci. *12*, 256–268.

Brosius, J. (1999). Many G-protein-coupled receptors are encoded by retrogenes. Trends Genet. *15*, 304–305.

Buck, L., and Axel, R. (1991). A novel multigene family may encode odorant receptors—a molecular basis for odor recognition. Cell *65*, 175–187.

Caterina, M.J., and Julius, D. (1999). Sense and specificity: a molecular identity for nociceptors. Curr. Opin. Neurobiol. *9*, 525–530.

Caterina, M.J., Schumacher, M.A., Tominaga, M., Rosen, T.A., Le-vine, J.D., and Julius, D. (1997). The capsaicin receptor: a heat-activated ion channel in the pain pathway. Nature *389*, 816–824.

Caterina, M.J., Leffler, A., Malmberg, A.B., Martin, W.J., Trafton, J., Petersen-Zeitz, K.R., Koltzenburg, M., Basbaum, A.I., and Julius, D. (2000). Impaired nociception and pain sensation in mice lacking the capsaicin receptor. Science *288*, 306–313.

Chandrashekar, J., Mueller, K.L., Hoon, M.A., Adler, E., Feng, L., Guo, W., Zuker, C.S., and Ryba, N.J. (2000). T2Rs function as bitter taste receptors. Cell *100*, 703–711.

Chen, A., and McConnell, S.K. (1995). Cleavage orientation and the asymmetric inheritance of Notch1 immunoreactivity in mammalian neurogenesis. Cell *82*, 631–641.

Dado, R.J., Law, P.Y., Loh, H.H., and Elde, R. (1993). Immunofluorescent identification of a delta (delta)-opioid receptor on primary afferent nerve terminals. Neuroreport *5*, 341–344.

Donaldson, L.F., Humphrey, P.S., Oldfield, S., Giblett, S., and Grubb, B.D. (2001). Expression and regulation of prostaglandin E receptor subtype mRNAs in rat sensory ganglia and spinal cord in response to peripheral inflammation. Prostaglandins Other Lipid Mediat. *63*, 109–122.

Dulac, C., and Axel, R. (1995). A novel family of genes encoding putative pheromone receptors in mammals. Cell *83*, 195–206.

Eddy, S.R. (1998). Profile hidden Markov models. Bioinformatics *14*, 755–763.

Elshourbagy, N.A., Ames, R.S., Fitzgerald, L.R., Foley, J.J., Chambers, J.K., Szekeres, P.G., Evans, N.A., Schmidt, D.B., Buckley, P.T., Dytko, G.M. (2000). Receptor for the pain modulatory neuropeptides FF and AF is an orphan G protein-coupled receptor. J. Biol. Chem. *275*, 25965–25971.

Friedel, R.H., Stubbusch, J., Barde, Y., and Schnurch, H. (2001). A novel 7-transmembrane receptor expressed in nerve growth factor-dependent sensory neurons. Mol. Cell. Neurosci. *17*, 31–40.

Fundin, B.T., Arvidsson, J., Aldskogius, H., Johansson, O., Rice, S.N., and Rice, F.L. (1997). Comprehensive immunofluorescence and lectin binding analysis of intervibrissal fur innervation in the mystacial pad of the rat. J. Comp. Neurol. *385*, 185–206.

Glusman, G., Yanai, I., Rubin, I., and Lancet, D. (2001). The complete human olfactory subgenome. Genome Research *11*, 685–702.

Goodier, J.L., Ostertag, E.M., and Kazazian, H.H. (2000). Transduction of 3′-flanking sequences is common in L1 retrotransposition. Hum. Mol. Genet. *9*, 653–657.

Gouarderes, C., Kar, S., and Zajac, J.M. (1996). Presence of neuropeptide FF receptors on primary afferent fibres of the rat spinal cord. Neuroscience *74*, 21–27.

Gouarderes, C., Roumy, M., Advokat, C., Jhamandas, K., and Zajac, J.M. (2000). Dual localization of neuropeptide FF receptors in the rat dorsal horn. Synapse *35*, 45–52.

Hinuma, S., Habata, Y., Fujii, R., Kawamata, Y., Hosoya, M., Fukusumi, S., Kitada, C., Masuo, Y., Asano, T., Matsumoto, H. (1998). A prolactin-releasing peptide in the brain. Nature *393*, 272–276.

Hinuma, S., Shintani, Y., Fukusumi, S., Iijima, N., Matsumoto, Y., Hosoya, M., Fujii, R., Watanabe, T., Kikuchi, K., Terao, Y. (2000). New neuropeptides containing carboxy-terminal RFamide and their receptor in mammals. Nat. Cell Biol. *2*, 703–708.

Hunt, S.P., and Mantyh, P.W. (2001). The molecular dynamics of pain control. Nat. Rev. Neurosci. *2*, 83–91.

I.H.G.S. (International Human Genome Sequencing Consortium). (2001). Initial sequencing and analysis of the human genome. Nature *409*, 860–921.

Jackman, A., and Fitzgerald, M. (2000). Development of peripheral hindlimb and central spinal cord innervation by subpopulations of dorsal root ganglion cells in the embryonic rat. J. Comp. Neurol. *418*, 281–298.

Jackson, T.R., Blair, L.A., Marshall, J., Goedert, M., and Hanley, M.R. (1988). The mas oncogene encodes an angiotensin receptor. Nature *335*, 437–440.

Kobilka, B. (1992). Adrenergic receptors as models for G protein-coupled receptors. Annu. Rev. Neurosci. *15*, 87–114.

Li, C., Kim, K., and Nelson, L.S. (1999). FMRFamide-related neuropeptide gene family in Caenorhabditis elegans. Brain Res. *848*, 26–34.

Ma, Q., Kintner, C., and Anderson, D.J. (1996). Identification of neurogenin, a vertebrate neuronal determination gene. Cell *87*, 43–52.

Ma, Q., Fode, C., Guillemot, F., and Anderson, D.J. (1999). NEUROGENIN1 and NEUROGENIN2 control two distinct waves of neurogenesis in developing dorsal root ganglia. Genes Dev. *13*, 1717–1728.

Malmberg, A.B., Chen, C., Tonegawa, S., and Basbaum, A.I. (1997). Preserved acute pain and reduced neuropathic pain in mice lacking PKCgamma. Science *278*, 279–283.

Matsunami, H., and Buck, L.B. (1997). A multigene family encoding a diverse array of putative pheromone receptors in mammals. Cell *90*, 775–784.

Matsunami, H., Montmayeur, J.P., and Buck, L.B. (2000). A family of candidate taste receptors in human and mouse. Nature *404*, 601–604.

McMahon, S.B., Armanini, M.P., Ling, L.H., and Phillips, H.S. (1994). Expression and coexpression of Trk receptors in subpopulations of adult primary sensory neurons projecting to identified peripheral targets. Neuron *12*, 1161–1171.

Michael, G.J., and Priestley, J.V. (1999). Differential expression of the mRNA for the vanilloid receptor subtype 1 in cells of the adult rat dorsal root and nodose ganglia and its downregulation by axotomy. J. Neurosci. *19*, 1844–1854.

Molliver, D.C., Wright, D.E., Leitner, M.L., Parsadanian, A.S., Doster, K., Wen, D., Yan, Q., and Snider, W.D. (1997). IB4-binding DRG neurons switch from NGF to GDNF dependence in early postnatal life. Neuron *19*, 849–861.

Mombaerts, P. (1999). Molecular biology of odorant receptors in vertebrates. Annu. Rev. Neurosci. *22*, 487–509.

Mombaerts, P., Wang, F., Dulac, C., Chao, S.K., Nemes, A., Mendelsohn, M., Edmondson, J., and Axel, R. (1996). Visualizing an olfactory sensory map. Cell *87*, 675–686.

Monnot, C., Weber, V., Stinnakre, J., Bihoreau, C., Teutsch, B., Corvol, P., and Clauser, E. (1991). Cloning and functional characterization of a novel mas-related gene, modulating intracellular angiotensin II actions. Mol. Endocrinol. *5*, 1477–1487.

Nelson, L.S., Rosoff, M.L., and Li, C. (1998). Disruption of a neuropeptide gene, flp-1, causes multiple behavioral defects in Caenorhabditis elegans. Science *281*, 1686–1690.

Offermanns, S., and Simon, M.I. (1995). G alpha 15 and G alpha 16 couple a wide variety of receptors to phospholipase C. J. Biol. Chem. *270*, 15175–15180.

Ohtaki, T., Shintani, Y., Honda, S., Matsumoto, H., Hori, A., Kanehashi, K., Terao, Y., Kumano, S., Takatsu, Y., Masuda, Y. (2001). Metastasis suppressor gene KiSS-1 encodes peptide ligand of a G-protein-coupled receptor. Nature *411*, 613–617.

Pantages, E., and Dulac, C. (2000). A novel family of candidate pheromone receptors in mammals. Neuron *28*, 835–845.

Panula, P., Kalso, E., Nieminen, M., Kontinen, V.K., Brandt, A., and Pertovaara, A. (1999). Neuropeptide FF and modulation of pain. Brain Res. *848*, 191–196.

Perez, S.E., Rebelo, S., and Anderson, D.J. (1999). Early specification of sensory neuron fate revealed by expression and function of neurogenins in the chick embryo. Development *126*, 1715–1728.

Perry, S.J., Yi-Kung Huang, E., Cronk, D., Bagust, J., Sharma, R., Walker, R.J., Wilson, S., and Burke, J.F. (1997). A human gene encoding morphine modulating peptides related to NPFF and FMRFamide. FEBS Lett. *409*, 426–430.

Price, D.A., and Greenberg, M.J. (1977). Structure of a molluscan carioexcitatory peptide. Science *197*, 670–671.

Rebeyrolles, S., Zajac, J.-M., and Roumy, M. (1996). Neuropeptide FF reverses the effect of mu-opioid on Ca2+ channels in rat spinal ganglion neurones. Neuroreport *7*, 2979–2981.

Rice, F.L., Fundin, B.T., Arvidsson, J., Aldskogius, H., and Johansson, O. (1997). Comprehensive immunofluorescence and lectin binding analysis of vibrissal follicle sinus complex innervation in the mystacial pad of the rat. J. Comp. Neurol. *385*, 149–184.

Ross, P.C., Figler, R.A., Corjay, M.H., Barber, C.M., Adam, N., Harcus, D.R., and Lynch, K.R. (1990). RTA, a candidate G protein-coupled receptor: cloning, sequencing, and tissue distribution. Proc. Natl. Acad. Sci. USA *87*, 3052–3056.

Scott, S.A. (1992). Sensory Neurons: Diversity, Development and Plasticity (Oxford: Oxford University Press).

Snider, W.D., and McMahon, S.B. (1998). Tackling pain at the source: new ideas about nociceptors. Neuron *20*, 629–632.

Snider, W.D., and Silos-Santiago, I. (1996). Dorsal root ganglion neurons require functional neurotrophin receptors for survival during development. Philos. Trans. R. Soc. Lond. B. Biol. Sci. *351*, 395–403.

Stucky, C.L., and Lewin, G.R. (1999). Isolectin B(4)-positive and -negative nociceptors are functionally distinct. J. Neurosci. *19*, 6497–6505.

Thompson, J.D., Higgins, D.G., and Gibson, T.J. (1994). CLUSTAL W: improving the sensitivity of progressive multiple sequence alignment through sequence weighting, position-specific gap penalties and weight matrix choice. Nucleic Acids Res. *22*, 4673–4680.

Tominaga, M., Caterina, M.J., Malmberg, A.B., Rosen, T.A., Gilbert, H., Skinner, K., Raumann, B.E., Basbaum, A.I., and Julius, D. (1998). The cloned capsaicin receptor integrates multiple pain-producing stimuli. Neuron *21*, 531–543.

Troemel, E.R., Chou, J.H., Dwyer, N.D., Colbert, H.A., and Bargmann, C.I. (1995). Divergent seven transmembrane receptors are candidate chemosensory receptors in C. elegans. Cell *83*, 207–218.

Tsien, R.Y., Rink, T.J., and Poenie, M. (1985). Measurement of cytosolic free Ca2+ in individual small cells using fluorescence microscopy with dual excitation wavelengths. Cell Calcium *6*, 145–157.

Venter, J.C., Adams, M.D., Myers, E.W., Li, P.W., Mural, R.J., Sutton, G.G., Smith, H.O., Yandell, M., Evans, C.A., Holt, R.A., et al. (2001). The sequence of the human genome. Science *291*, 1304–1351.

Vilim, F.S., Aarnisalo, A.A., Nieminen, M.L., Lintunen, M., Karlstedt, K., Kontinen, V.K., Kalso, E., States, B., Panula, P., and Ziff, E. (1999). Gene for pain modulatory neuropeptide NPFF: induction in spinal cord by noxious stimuli. Mol. Pharmacol. *55*, 804–811.

Wang, F., Nemes, A., Mendelsohn, M., and Axel, R. (1998). Odorant receptors govern the formation of a precise topographic map. Cell *93*, 47–60.

Willis, W.D., and Coggeshall, R.E. (1991). Sensory Mechanisms of the Spinal Cord (New York: Plenum Press).

Xie, S.Y., Feinstein, P., and Mombaerts, P. (2000). Characterization of a cluster comprising approximately 100 odorant receptor genes in mouse. Mamm. Genome *11*, 1070–1078.

Young, D., Waitches, G., Birchmeier, C., Fasano, O., and Wigler, M. (1986). Isolation and characterization of a new cellular oncogene encoding a protein with multiple potential transmembrane domains. Cell *45*, 711–719.

Zhao, H., Ivic, L., Otaki, J.M., Hashimoto, M., Mikoshiba, K., and Firestein, S. (1998). Functional expression of a mammalian odorant receptor. Science *279*, 237–242.

Accession Numbers